Time-resolved Transillumination For Medical Diagnostics

Andersson-Engels, Stefan; Berg, R; Svanberg, Sune; Jarlman, O

Published in:
Optics Letters

DOI:
10.1364/OL.15.001179

1990

Time-resolved transillumination for medical diagnostics

S. Andersson-Engels, R. Berg, and S. Svanberg

Department of Physics, Lund Institute of Technology, P.O. Box 118, S-221 00, Lund, Sweden

O. Jarlman

Department of Diagnostic Radiology, Lund University Hospital, S-221 85, Lund, Sweden

Received April 26, 1990; accepted August 31, 1990

A time-gated technique to improve the possibility of localizing spatial differences in absorption when transilluminating a turbid, highly scattering medium, such as human tissue, is demonstrated. When transmitting picosecond laser pulses and detecting photons on the opposite side of the object, the contrast can be strongly enhanced by detecting only the photons with the shortest traveling time. Measurements on a 35-mm-thick tissue phantom with 5-mm-diameter absorbing objects inside are reported with data for a human hand *in vivo*. Implications for optical mammography (diaphanography) are discussed.

Today mammography is the golden standard in breast cancer diagnosis. However, tumors sometimes cannot be seen, especially in a dense breast, and the use of ionizing radiation is also a matter of concern since there is a hypothetical risk of cancer induction, especially in young women. Tissue transillumination is a diagnostic modality based on the characteristic absorption of light in malignant tumors owing to the surrounding neovascularization.[1–3] In optical transillumination, wavelengths with low absorption in tissue, i.e., red or near-infrared light, have to be used.[4] The main problem is that in this wavelength region the dominating attenuating effect is not absorption but scattering.[5] The scattering coefficient is of the order of 10 mm^{-1}, while the absorption coefficient is of the order of 0.1 mm^{-1}.[6] The large scattering coefficient induces pronounced multiple scattering in the tissue.[7,8] This effect causes a decreased contrast when breast transillumination is performed.[9] Different methods to reduce the effect of light scattering have been suggested.[10–12] In this Letter a time-gating technique to do this is demonstrated.

The time-gating technique is based on the concept that light which leaves the transilluminated breast earlier has traveled a shorter and straighter path in the tissue than light exiting later. This early light is less scattered and thus contains more information about the spatial localization of the absorption, which in this case means the localization of the tumor. Such a technique has been analyzed theoretically by Maarek *et al.*[13]

In this Letter we describe experiments on a tissue-like phantom and a hand *in vivo* to investigate the increase in contrast when the time-gating technique is used in a highly scattering medium. The first demonstration using a solid object in a scattering liquid was presented in Ref. 14.

Figure 1 shows the experimental setup. The light source was a mode-locked Coherent CR-3000K Ar-ion laser pumping a Coherent CR-599 dye laser equipped with a cavity dumper. The pulses from the dye laser were measured and evaluated to be 8 psec (FWHM) wide by using an autocorrelator. The average output power was 50 mW at the chosen wavelength of 630 nm, and the repetition frequency was approximately 5 MHz. The laser pulses irradiated the object, and the light was detected on the opposite side. The detector assembly consists of a small (<1-mm) aperture and a lens that focuses the light onto a 600-μm optical fiber. The acceptance angle for the detector is 2°, i.e., the light can enter the detector only if the angle is less than 1° off the optical axis. To achieve time-resolved detection, delayed coincidence techniques were used. The detector fiber is connected to a photon-counting multichannel plate (Hamamatsu 1564U-07), and the

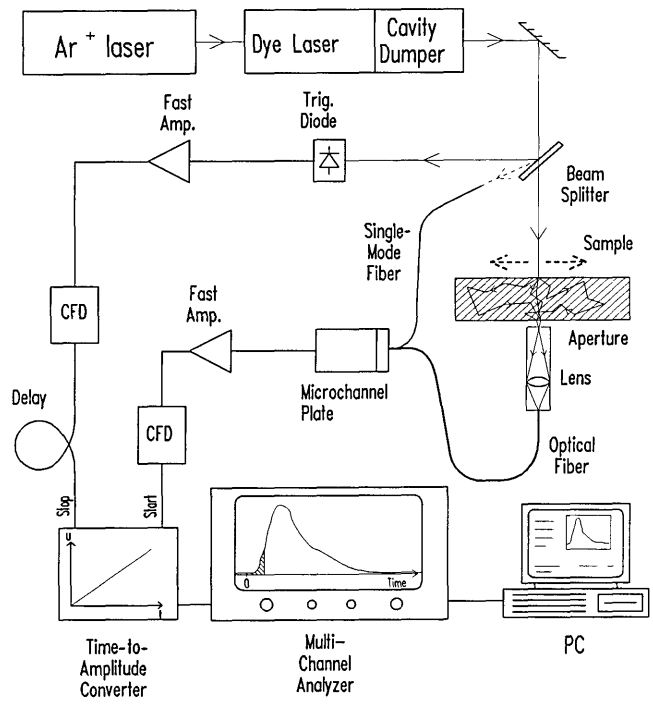

Fig. 1. Experimental setup.

0146-9592/90/211179-03$2.00/0

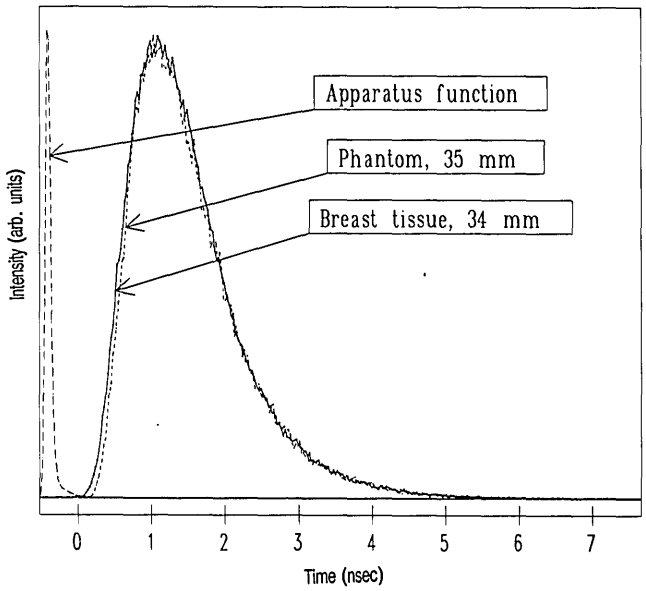

Fig. 2. Typical detected time-dispersion curves. The dotted curve shows the dispersion curve obtained when transilluminating the 35-mm-thick paraffin phantom. The solid curve shows the result when transilluminating a 34-mm-thick breast sample *in vitro* 1 h postmastectomy. The impulse response function of the system (apparatus function) is also given.

signal is fed through a fast amplifier and a constant fraction discriminator (CFD) to a time-to-amplitude converter. This signal is the start signal for the time-to-amplitude converter. The stop signal comes from a diode triggering on the incident pulse. The trigger pulse is also fed through a fast amplifier and a CFD. The output signal from the time-to-amplitude converter is fed to a multichannel analyzer in which a histogram of arrival time for the photons is formed, i.e., the temporal dispersion curve. The curves can be transferred to a computer (PC) for evaluation. The impulse response function for this system is approximately 80 psec (FWHM). The impulse response is shown in Fig. 2. The experimental setup and the evaluation procedure are discussed in more detail in Ref. 15.

In order to ensure a well-defined measurement situation, experiments were performed on a tissue phantom, which was a block of paraffin. The dimensions of the paraffin were 150 mm × 55 mm × 35 mm, and thus the minimum optical path length was 35 mm. In Fig. 2 a comparison between the temporal dispersion curves for real breast *in vitro* and the phantom tissue can be seen. The solid curve shows the result when transilluminating a 34-mm-thick sample of breast tissue 1 h postmastectomy. The dotted curve shows the temporal dispersion curve obtained with the 35-mm-thick phantom. As can be seen, the curves are similar, and thus the phantom should be a good substitute for real tissue in this experiment. A considerable fraction of the light exits more than 3 nsec after the first transmitted light, which corresponds to an effective path length of more than 60 cm owing to heavy multiple scattering. Five holes were drilled into the phantom perpendicularly to the laser beam–detector plane. Pieces of black rubber cord were inserted into the holes to simulate ideal totally absorbing tumors. Figure 3 (top) shows the phantom. The cords are 5 mm in diameter and located 5.5, 11.5, 17.5, 23.5, and 29.5 mm from the surface that is closest to the laser beam. The phantom can be translated across the beam–detector axis, and scanning can thus be performed. A temporal dispersion curve was sampled for 60 sec for every millimeter from 0 to 100 mm. To permit comparison of the different dispersion curves, a time-reference peak was obtained with every curve. That is, a single-mode optical fiber of suitable length was connected to the multichannel plate to detect a small part of the input pulse and thus create an impulse response peak in front of every dispersion curve, and this peak thus formed a reference in time. Before evaluation the curves were deconvoluted with the impulse response function to increase the effective time resolution. Figure 3 (bottom) shows the result of the scanning. The dashed curve shows all the detected light, i.e., the integral of the dispersion curves. The solid curve shows the amount of light detected early. The early light is the light detected during the first 100 psec of the dispersion curve. This corresponds to five channels in the multichannel analyzer. The width of the early light window is a compromise between the contrast and the signal-to-noise ratio. The wider the window the better the signal-to-noise ratio but the lower the contrast. A window of 100 psec corresponds to a distance 0.6 times the thickness of the phantom,

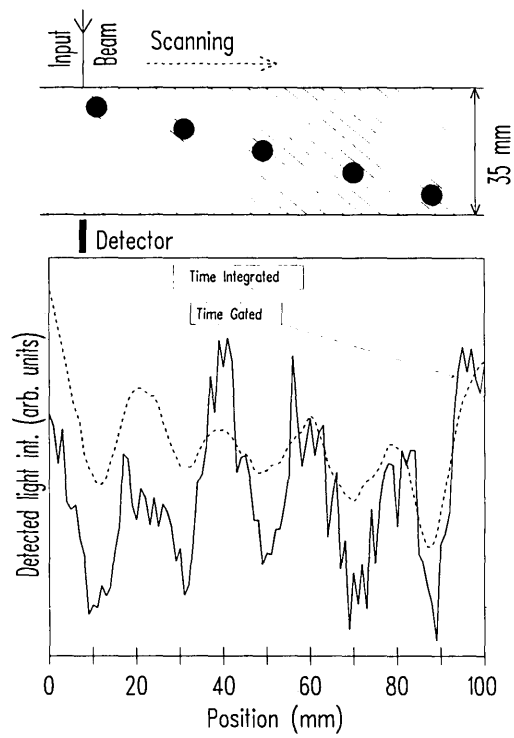

Fig. 3. (Top) Sketch of the paraffin phantom with pieces of black rubber cord inserted into it. (Bottom) Detected light intensity when scanning over the phantom with a resolution of 1 mm. The solid curve shows the result when light is detected the first 100 psec of every dispersion curve, i.e., the time-gated technique. The dashed curve shows the total amount of light detected at each point. The curves are arbitrarily normalized.

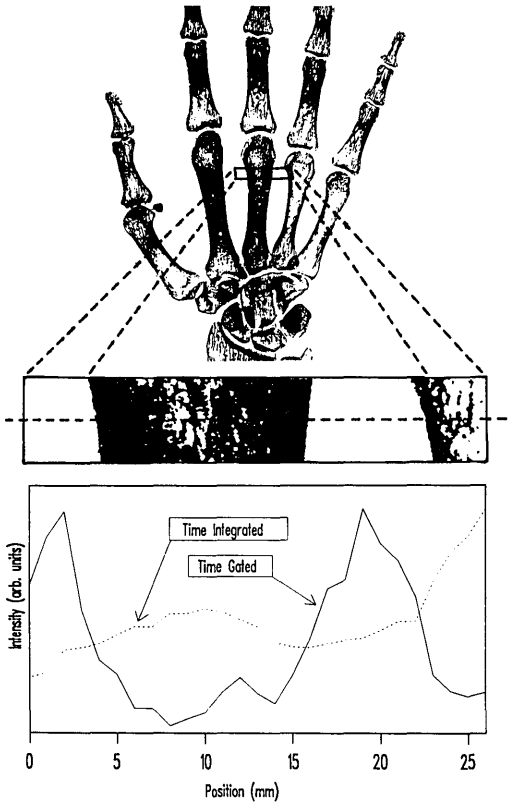

Fig. 4. Detected light intensity when scanning across a hand *in vivo*. The solid curve corresponds to the light detected during the first 80 psec, and the dotted curve is the total detected light.

calculated with a medium refractive index of 1.4. Thus the light detected with the time-gated technique is determined by a weighted average absorption over a volume of the phantom. The difference is that with the time-gated technique this volume is much smaller and more localized. The probability of detecting light that has traveled across the phantom without being scattered at all is almost zero, since the mean free path length for the photons is of the order of 100 μm. A test with polarization as a discriminating criterion verified this. If some of the light is not scattered, there should be a difference in the amount of vertically and horizontally polarized light exiting since the input pulse is vertically polarized, but the light exiting the phantom was totally unpolarized, even the detected early photons.

As can be seen in Fig. 3, there is an increase in contrast when the early light method is utilized. The contrast is defined as $C = (I_2 - I_1)/(I_1 + I_2)$, where I_1 is the amount of light detected with a cord between the laser beam and the detector and I_2 is the amount of light detected with no cord between the laser beam and the detector. The contrast varies for the time-gated case between approximately 0.5 and 0.8. The contrast for the total detected light is 0.1–0.3. The improvement in contrast is better than 2.5 times for all the pieces of cord. The figures also show that the contrast is much less dependent on the position of the cord in the phantom.

A similar scan was also carried out across a human hand *in vivo*. The results are shown in Fig. 4. The solid curve corresponds to the light intensity detected during the first 80 psec, and the dotted curve shows the total amount of light detected. The scan was performed approximately 10 mm below the knuckle of the middle finger. As can be seen in Fig. 4 there is a significant demarcation of the bones. It can also be seen that the two curves are out of phase. This phenomenon still needs to be investigated.

In summary, when performing transillumination of a turbid, highly scattering medium such as tissue for the purpose of detecting spatial variations in absorption, we have shown that the time-gating technique can be used to improve the result. To be able to use this technique for malignant tumor detection in the female breast, an imaging system should be used. We are planning the development of such a technique as well as spectroscopic recordings for evaluating optimal wavelengths to obtain the best contrast between malignant tumors and healthy breast tissue. Such spectral differences are much enhanced when using the time-gated technique since the attenuation due to absorption is then favored over attentuation due to scattering.

Valuable discussions with L. O. Svaasand and skillful help from Jonas Johansson are gratefully acknowledged. This research was supported by the Swedish Board for Technical Developments.

References

1. B. Ohlsson, J. Gundersen, and D.-M. Nilsson, World J. Surg. **4**, 701 (1980).
2. D. J. Watmough, Radiology **147**, 89 (1983).
3. B. Drexler, J. L. Davis, and G. Schofield, Radiology **157**, 41 (1985).
4. S. Ertefai and A. E. Profio, Med. Phys. **12**, 393 (1985).
5. B. C. Wilson, M. S. Patterson, S. T. Flock, and D. R. Wyman, in *Photon Migration in Tissue*, B. Chance, ed. (Plenum, New York, 1989).
6. R. Marchesini, A. Bertoni, S. Andreola, E. Melloni, and A. E. Sichirollo, Appl. Opt. **28**, 2318 (1989).
7. M. S. Patterson, B. Chance, and B. C. Wilson, Appl. Opt. **28**, 2331 (1989).
8. D. T. Delpy, M. Cope, P. van der Zee, S. Arridge, S. Wray, and J. Wyatt, Phys. Med. Biol. **33**, 1433 (1988).
9. G. A. Navarro and A. E. Profio, Med. Phys. **15**, 181 (1988).
10. K. G. Spears, J. Serafin, N. H. Abramson, X. Zhu, and H. Bjelkhagen, IEEE Trans. Biomed. Eng. **36**, 1210 (1989).
11. P. P. Ho, P. Baldeck, K. S. Wong, K. M. Yoo, D. Lee, and R. R. Alfano, Appl. Opt. **28**, 2304 (1989).
12. M. Toida, T. Ichimura, and H. Inaba, in *Conference on Lasers and Electro-Optics*, Vol. 7 of OSA Technical Digest Series (Optical Society of America, Washington, D.C., 1990), pp. 548–550.
13. J. M. Maarek, G. Jarry, J. Crowe, M.-H. Bui, and D. Laurent, Med. Biol. Eng. Comput. **24**, 407 (1986).
14. S. Andersson-Engels, R. Berg, J. Johansson, K. Svanberg, and S. Svanberg, in *Laser Spectroscopy IX*, M. Feld, ed. (Academic, New York, 1989), pp. 500–504.
15. R. Berg, M.S. thesis, Lund Reports on Atomic Physics LRAP-106 (Lund Institute of Technology, Lund, Sweden, 1989).